Ray-tracing MRT and human thermophysiology model combination for local discomfort prediction

Mohamad Rida [a], *Miaomiao Hou* [c,b], *Arnab Chatterjee* [a], *Eric Teitelbaum* [d], *Forrest Meggers* [d], *Dorit Aviv* [b], *Dolaana Khovalyg* [a].

[a] Integrated Comfort Engineering (ICE), Ecole Polytechnique Fédérale de Lausanne (EPFL), Switzerland.

[b] Thermal Architecture Lab (TAL), Weitzman School of Design, University of Pennsylvania, USA.

[c] College of Architecture and Urban Planning, Tongji University, China.

[d] CHAOS Lab, Andlinger Center for Energy and the Environment, Princeton University, Princeton, NJ, USA.

Abstract. Thermal comfort and discomfort based on the local sensation of different body parts have been an important development in thermal comfort studies from the past decade. The human thermophysiology model can be a handy tool to predict local skin and core temperatures, which can then be projected into diverse human's local and overall thermal sensation and comfort. When local environmental parameters are incorporated in the thermophysiology model, the degree of modeling information improves. One of the important input parameters is the mean radiant temperature. Variations in radiant heat fluxes when shortwave radiation is present in the room can be significant. Combining novel scanning and thermography methods together with ray-tracing simulation, we derived a high-resolution thermal model to fully characterize the variations of radiant heat fluxes experienced by different body parts of a human, both longwave (LW) and shortwave (SW). The shortwave heat flux varied in the range of 0-216 W/m2 throughout the day in the experiments conducted in an office room prototype on 23/02/2021 in Fribourg, Switzerland. The radiant temperature experienced by different body parts varied widely, from 24 °C to 58 °C, due to uneven exposure to solar radiation through a window, while the air temperature remained relatively uniform, as it was controlled by a mechanical system. To demonstrate the importance of combining detailed MRT modeling together with the thermophysiology model, we input detailed MRT distribution into the human thermophysiology model, along with the environmental parameters from the experimental measurements. The calculated skin temperatures were compared with the measured ones using iButtons and thermal sensation and comfort values with the survey results collected from the human subject. A combination of these detailed methods can be used as a design tool to assess local (dis)comfort and thermal perception of an occupant exposed to shortwave radiation and for dynamic shading and personalized comfort systems control strategies.

Keywords. Solar radiation, Local MRT, Human thermal comfort, Human thermo-physiology.
DOI: https://doi.org/10.34641/clima.2022.371

1. Introduction

Even in a well-conditioned building, our thermal environment is frequently transient and non-uniform because of the different zonal environments and the solar radiation propagated through the windows. The determination of microclimate conditions of a person inside a space is required in order to achieve a high standard thermal comfort quality in the space where the human activity is undertaken.

Solar radiation passing through a transparent construction has a significant impact on thermal comfort and the indoor thermal environment. Consequently, unshaded windows exposed to excessive sun irradiation can cause overheating as well as undesirable thermal environments in particular areas of the interior space [1]. The massive use of glass as an architectural component in modern buildings, as well as the associated solar radiation, leads to an increase in serious indoor thermal discomfort issues [2]. In contrast, the primary premise of passive solar designs is to increase the use

of solar gain and day lighting in order to reduce the energy used for heating during the winter season without compromising the occupant's thermal comfort. Otherwise, people usually react to the thermal discomfort from the solar radiation by pulling the shading system ON if they have control over it . Finally, indoor thermal comfort in buildings with a large glazing façade is heavily dependent on the direct component of solar radiation on the human body [3].

The Predicted Mean Vote (PMV) established by Fanger is generally used to predict persons' thermal sensation and has been included in the ISO7730 standard [4]. Solar radiation, on the other hand, was not taken into consideration in Fanger's PMV where only the long-wave radiation heat transfer between humans and surroundings is considered. The average values of microclimatic environmental parameters are commonly used to assess occupant global thermal comfort conditions. However, in many situations, the preceding approach does not result in an accurate assessment of individual environmental quality because the variability of environmental parameters around the human body, as well as its transient nature, should be considered in the assessment.

The short-wave radiation fell on the human body has a heating effect, which lead to an increase of the outer surface temperature of the human body and consequently, leads to local warm sensation. Furthermore, local thermal discomfort that is happening due to unpleasant local heating or cooling of a particular area of the body can lead to global thermal discomfort [5]. This can be mainly caused by the stratification height, a high variation in vertical temperature, a large and significant air draft, or radiant asymmetry. The human thermal sensation is the person's thermal perception of the environment, which is related to the local environmental parameters, personal parameters specified as activity level and clothing insulation, as well as the specific body composition such as gender, body fat and BMI.

Therefore, approaches that address this issue require the use of thermophysiological models that can predict human thermal response as a function of both physiological factors and variables that define the surrounding thermal environment. A detailed human thermal model (HTPM) is usually used in order to address the variability in the local thermal environment over the body parts. These models are capable of assessing the skin temperature dynamically as well as other physiological responses. Local skin temperature is the main factor to evaluate in order to project a person's local thermal sensation. HTPMs represent the thermodynamics of human body interaction with the environment and are defined as a set of energy balance equations at each layer of a body segment. These models take the local environmental parameters as inputs, and it's up to the modeller to either consider a uniform or non-uniform environment based on the studied situation. Direct solar radiation on separate body parts is rarely accounted for, but some researchers considered it in the calculation of mean radiant temperature [6], while others used the heat flux directly to the corresponding body part [7].

The multi-node multi-segment HTPM segments the human body into multiple body parts, each part in multiple concentric layers, and all body parts are connected by a blood circulatory system [7-11]. All these models were initially based on the model of Stolwijk [12]. Taking the radiant asymmetric factor into account increases the detailed level of modelling. Furthermore, the results predicted are highly dependent on the subject's posture, the position of the person inside the spaces as well as other individual physiological factors which are variable among individuals. Individual variability has been accounted for in some models such as [7,9]. The contribution of solar radiation to the global thermal comfort and local thermal comfort conditions for a person sitting near a glass window in a building is sometimes underestimated. In this study, the effects of transmitted direct solar radiation, transmitted diffuse solar radiation, inside glass surface temperature, as well as all surrounding surface temperatures have been considered to calculate the local MRT distribution on a 3D scanned human body. A detailed human thermo-physiology model has been used to predict the local skin temperatures, which has been compared with the experimental results. Moreover, a local thermal sensation has been projected based on the person's thermal state from the HTPM simulation.

2. Methodology

The purpose of the simulation is to propose a method that can be relied upon in the design of comfortable indoor spaces where glass and non-opaque facades exist. Solar radiation can be a source of discomfort, especially in warm weather.

We can reduce the number of measurements required by simulating the real-world scenario, especially those that require the person to wear a sensor or answer surveys.

Finding the human local and overall thermal sensation can be achieved by the use of a detailed thermo-physiology model combined with a detailed thermal sensation model.

2.1 Experimental setup

The experiment has been conducted in a facility which can be described as a 1-story office building, that consists of two geometrically identical rooms. The rooms' dimensions are 3.07m width x 6.23m length x 3.10m height. Each room has two double-glazed windows of 2.52m width x 1.83m height, one window is facing north and the other facing south.

The overall U-value of the opaque walls is 0.139 w/m2k, and the windows has a g-value 65%, and average transmittance of 36% over 285-3000nm. Each window has an internal textile roller blind as well as an external Venetian blind.

The room has three radiant ceiling panels. Each panel has the following dimensions of 0.33 m x 3.75 m, and the distance between the panels is 0.31 m. The fresh air is supplied through a circular diffuser located on the east wall with a flow rate of 68.5 m3/h.

2.2 Personal and environmental parameters

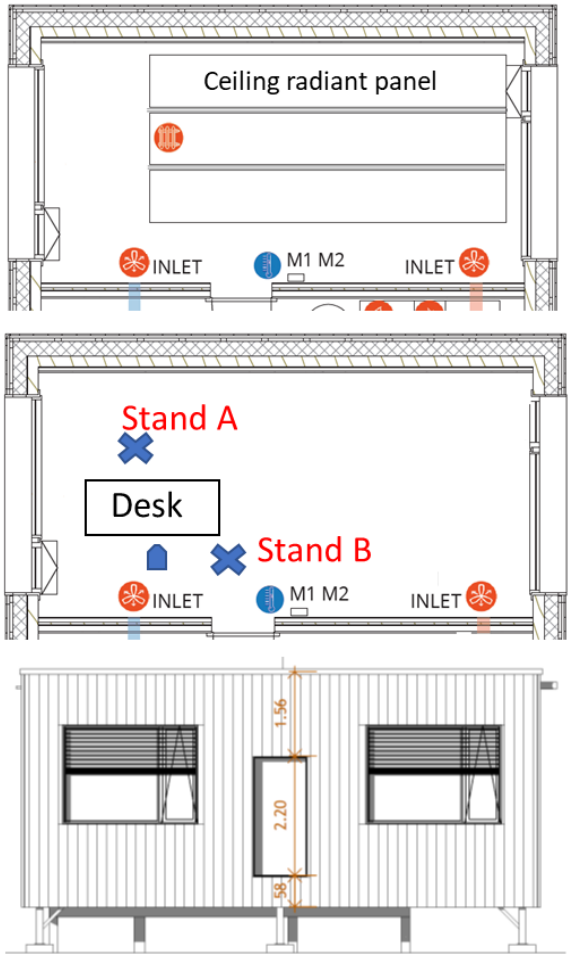

Fig. 1- Representation of the experimental set-up and an exterior and interior image of the facility.

In the experiment, multiple environmental sensors were used. The SPN1 pyranometer (Delta-T, UK) was used to measure outdoor direct, normal, and diffuse horizontal irradiance with an accuracy of ±10 W/m2. The dry bulb temperature and air speed were measured every second on two vertical stands 0.2 m distant from the right of the subject, and 1.2m in front-left of the subject, as shown in Figure 1, and at four different heights (0.1, 0.6, 1.1, 1.7 m), and relative humidity was measured in the centre of the room. Figure 1 depicts the general configuration of the room's environmental sensors as well as an exterior and interior schematic of the facility.

To improve the accuracy of radiant temperature readings, two digital, non-contact longwave measuring equipment were employed. The Scanning Mean Radiant Temperature (SMART) Sensor is a spatially resolved thermal imager that consists of a melexis 90614 five-degree field of view non-contacting medical grade surface temperature sensor (accuracy 0.5°C) and a Garmin LidarLite module (2 cm over 40 m). The sensor rotates on perpendicular axes and records the angular position of the servos, which are then rebuilt using Lidar and temperature data to build a thermal point cloud of the surface temperatures in the scanned area.

The temperature of the skin was recorded at 24 positions of the body, iButton® temperature loggers DS1922L were used (MAXIM Integrated, USA) which has an accuracy of 0.25°C. 14 out of the 24 sensors position were chosen as recommended in the standard ISO 9886:2004 which can be used to do the 14-point weighting scheme. The other locations were used to check the differentiation between left and right. Figure 2 presents a schematic of the skin temperature sensor's position on the human body. During the experiment the subject was wearing a short-sleeve T-shirt, denim pants, sneakers, ankle socks, and underwear with an overall clothing insulation of 0.57 clo.

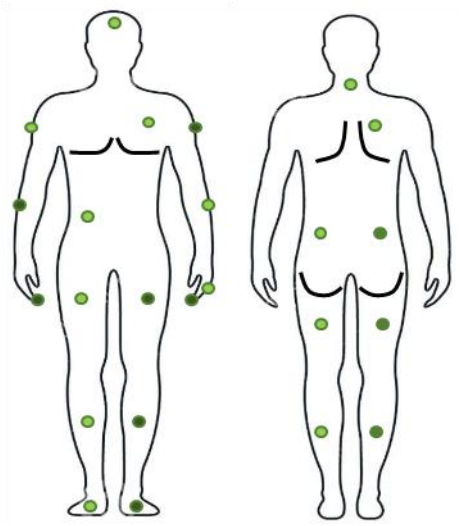

Fig. 2- skin temperature sensor location front and back and image of the subject during the experiment.

The metabolic rate was considered to be 1.2-1.4 met as the person was sitting performing office work. The variation in metabolic rate between the morning and afternoon was considered in addition to the effects of brake activity.

The subject body compositions are stated in table 1.

Tab. 1 - The subject's body composition.

Sex	Age	Hight (m)	Weight (kg)	Fat Percent. %	Body surf. area (m^2)
M	29	1.75	72.9	28.2	1.98

2.3 Experimental scenarios

The averaged environmental parameters of the three experimental scenarios are presented in table 2. The three scenarios can be described as follows, in all the three experiments the blinds of the north window were set down. The blinds were kept up in the south window for both experiment I and II but were down in experiment III. In each experiment the subject was sitting for one hour during each session the SMART sensor scans all the surfaces twice (once every half-hour). The three experiments were conducted during one day and the time of each session is shown in table 3.

Tab. 2 - The inputs of the parameters for the PMV thermal comfort model.

	Exp I		Exp II		Exp III	
T_air (°C)	23.3	24	25.1	26	24.7	24.5
V_air (m/s)	0.05	0.05	0.1	0.1	0.04	0.05
RH %	25	25	21	22	23	24

Tab. 3 - Time of the experiments in the day

	Session	Time of the day
Exp I	a	10:17-10:47
	b	10:52-11:22
Exp II	a	13:12-13:42
	b	13:47-14:17
Exp III	a	15:34-16:04
	b	16:15-16:45

2.4 Simulation setup

In this study we chose to consider local air temperature and air velocity data measured from the experiment although those values could be calculated through a CFD model.

Three separate sessions have been performed in the experiment, where all measured skin temperature data has been compared to simulation results. In the simulation, the initial conditions are always required, and to simplify, we ran the HTPM model over the whole day, considering that breaks are conducted in a uniform environment of 25°C operative temperature.

2.5 Local air temperature

In the simulation we took the detailed air temperature distribution from the experimental results at four different heights to assign the local body air temperatures. Local air temperature was measured in the experiment using two poles located to the subject's right and front left. Figure 3 shows the air temperature corresponding to each body part.

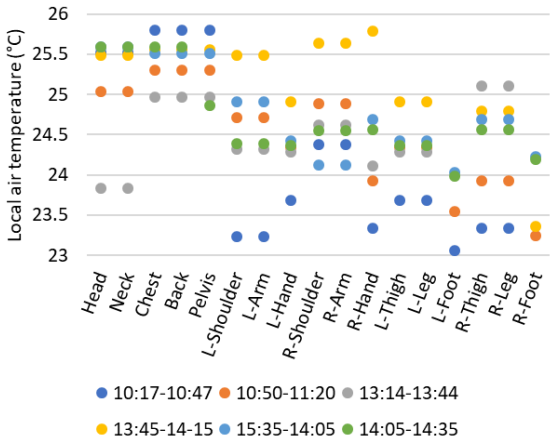

Fig 3- Local air temperature

2.6 Mean radiant temperature

The local mean radiant temperature was calculated through a sophisticated ray-tracing method in the Grasshopper algorithmic modelling tool within the Rhino 3D environment, allowing for five-phase radiation bounces within the room. The radiant heat transfer model accounts for the interreflections from room surfaces with the use of high-resolution geometric models combined with material properties and surface temperature of all exposed surfaces in the room. For each test point on the body surface, heat flux vectors emanating from the point are traced through bounces, during which the radiant heat exchange at each intersection with the surrounding surfaces can be calculated. The details of this method can be found in our previous papers [13].

The 3D room mesh model was built in Rhino with a 0.1 m × 0.1 m grid size. The human 3D body model was obtained from performing a 3D scan and subdivided into 3,916 surfaces based on the 17 segments used in the thermo-physiology model. The reflectivity of the main surfaces indoors can be different for shortwave or longwave radiation, e.g. floor-0.05 for LW, 0.16 for SW; wall and ceiling-0.1 for LW, 0.7 for SW. The transmittance of the glazing that allows solar radiation coming in is 0.36.

The simulation contains shortwave and longwave components, which need different inputs. For the longwave irradiance simulation, the surface temperature was majorly measured with a high-resolution thermal array scanning and mapping platform named SMART [15], which can spatially resolve surface temperature into 3D thermal point clouds. Together with the use of thermocouples and

thermography, surface temperature of all exposed surfaces were obtained and connected to the geometric model in a 3D environment. The body skin and clothes temperature were measured with wearable temperature sensors and the surface temperature of the clothed body of 14 locations were used to create the body temperature mesh. In the shortwave component, an environmental plugin in Grasshopper named Honeybee was used to calculate the shortwave irradiance on every body surface of a specific date and time with additional inputs of geographic location and measured solar irradiance.

For each body surface, the radiant temperature can be derived from the combination of shortwave and longwave portions. The radiant temperature of smaller segments varied from 24.8 to 58.5 °C across the body, and the range was narrowed to 26.4-43.1°C when averaging the data of small segments within every one of the 17 segments. Figure 4a shows the local mean radiant temperature of the 17 body parts, which correspond with the body part segmentation shown in Figure 2. The areas exposed to direct sunlight from the left, e.g. left side of the head, abdomen and both arms, had significantly higher radiant temperature than other parts. By averaging the radiant temperature of all segments with the surface area of the segments as weighted coefficients, the whole-body MRT can be calculated. The human subject had the highest MRT above 33 °C in the second session and the lowest in the third session, as is shown in Figure 4b.

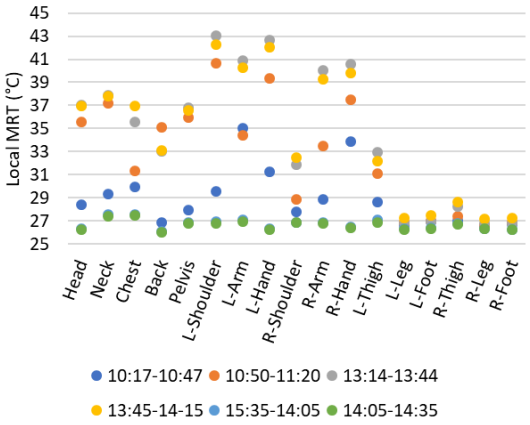

Fig 4b- Local radiant temperature for different segments at different time steps

2.4 Human thermo-physiology model

In this study we have adopted the human thermo-physiology model JOS3 as an open source model developed by [7]. The model initially includes 17 body parts including the head, neck, chest, back, pelvis, right and left shoulders, arms, hands, thighs, legs, and feet. We have further improved the model to account for the 10 fingers. The model is personalized by taking the age, gender, height, weight and body fat of each subject into account. As mentioned in Table 1 all the body composition has been considered in the simulation. By evaluating the local (Tskin,i) and mean skin temperature (Tskin,mean) output from the HTPM, we can project

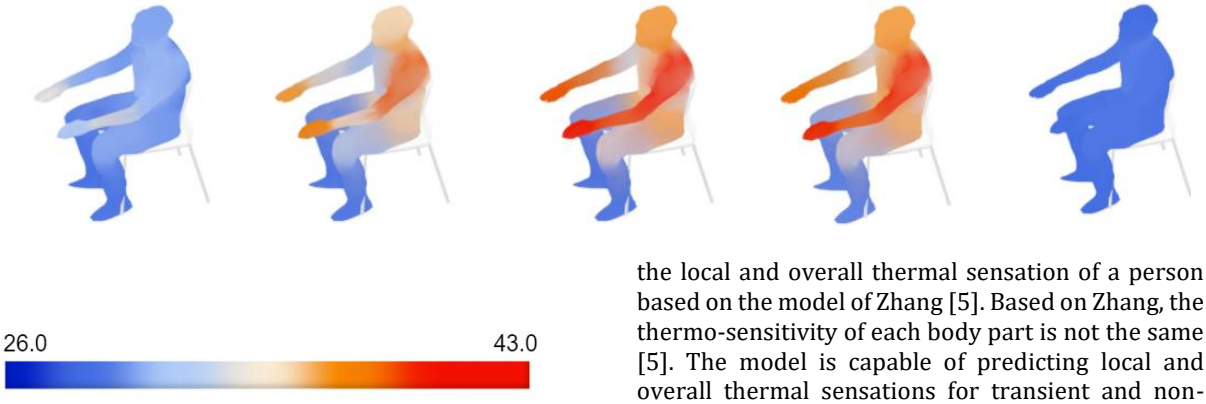

Fig 4a- Illustration showing body segment planar radiant temperature variations during the experiments

the local and overall thermal sensation of a person based on the model of Zhang [5]. Based on Zhang, the thermo-sensitivity of each body part is not the same [5]. The model is capable of predicting local and overall thermal sensations for transient and non-uniform environments. Where the local sensation is a function of local skin temperature and is given by the following equation:

$$S_{body\ seg} = 4 * \left(\frac{2}{1+e^{-C_1\left(T_{part,skin}-Tset_{part,skin}\right)-K_1\left[\left(T_{part,skin}-T_{mean,skin}\right)-\left(Tset_{part,skin}-Tset_{mean,skin}\right)\right]}} - 1 \right) + C_{2i}\frac{dT_{part,skin}}{dt} + C_{3i}\frac{dT_{core}}{dt}$$

Where S is the local sensation and $body\ part\ C$ are cold and warm coefficients 1, $K1$, $C2i$ *and* $C3i$ based on Zahng's model [12].

3. Results

3.1 Local and mean skin temperature

To evaluate our simulation results, we have compared the mean skin temperature along with the local skin temperatures to the measured ones from the experiment. As mentioned previously, three different sessions represent three different times of the day with different solar radiation intensities affecting the subject. Figure 5 represents the temperature comparison between the simulation and experimental data. The figure has 6 sub-figures, each representing the data corresponding to one experimental set-up. From the results, we can see that the thermo-physiology prediction showed some agreement with the experimental results in multiple body parts. Where the head skin temperature showed an acceptable agreement, especially in the first and last sessions, in the second session the difference exceeded one degree centigrade. The hand skin temperature showed good agreement in the second session but deviated at the end of the first session as well as in the third session, where results showed the largest discrepancy. The shoulder skin temperature showed acceptable agreement in the second and third sessions, but differences were greater in the first session. In general, the mean skin temperature, on the other hand, was acceptable in the three sessions, with less than 0.5°C in the third session and the highest discrepancy of around 1°C in the second session.

Those differences could be due to multiple reasons, where the most come from the detailed physiology model, since the physiology model considers a generalised physiological set point and we are comparing it to one specific subject. Secondly, the MRT calculation has been conducted on a half-hour basis and it is considered constant in the simulation during that time.

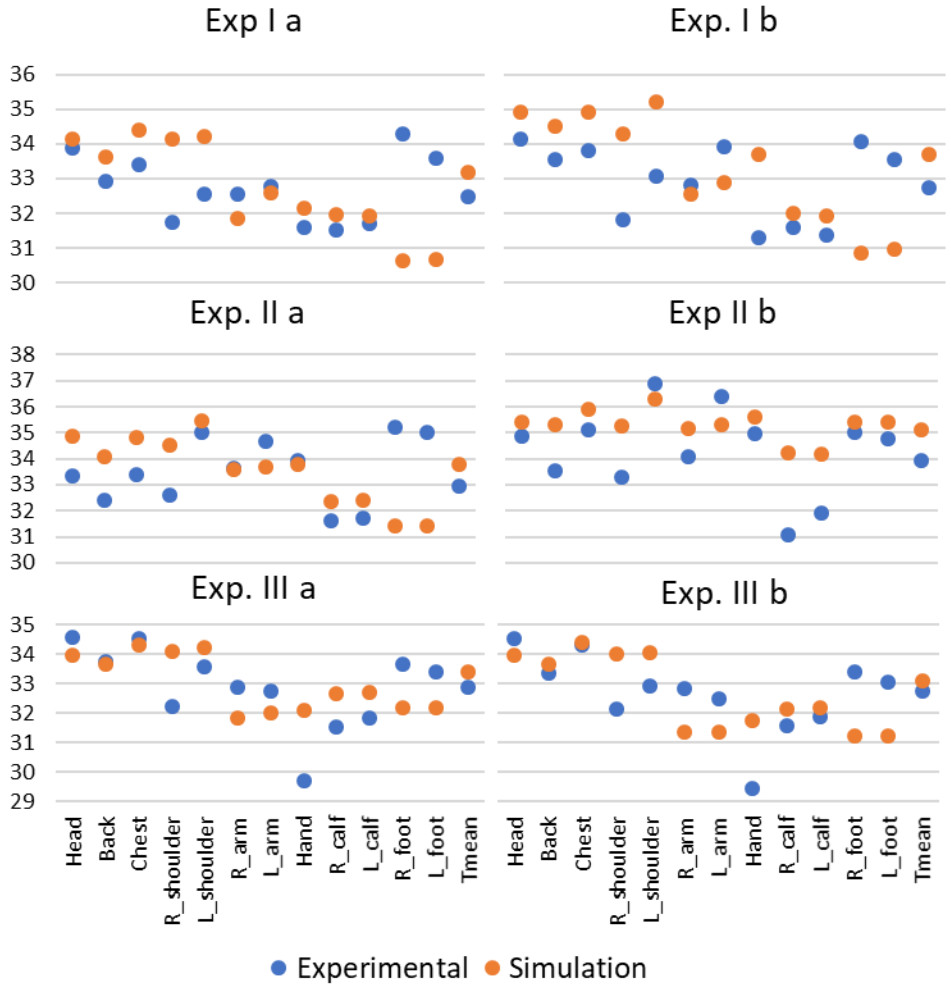

Fig 5- Experimental vs. simulation results at different body parts

4.2 Local and overall sensation

The physiology model has been linked to a detailed local sensation model of Zhang (2010). The results from the model showed that during the first session when MRT showed elevated values in the second half-hour of the session reached 31 °C, the overall sensation increased from neutral to warm with a value of 2 on the 9-point scale. In the second session, MRT was high during the whole period, and that was reflected in the overall sensation with a value of +3,

which corresponds to "Hot". As for the third session, the solar radiation was almost negligible, with MRT values fluctuating around 1°C higher than the air temperature, the overall sensation was in the neutral range. Looking at the local sensation values as Figure 6 shows, the sensation of the head was the highest and the most sensitive body part toward the elevated temperature. The differences between the left and right can be seen in the shoulders, where sensation has higher values for the left shoulder, especially during exposure to solar radiation. The difference in sensation between the left and right shoulders was around one point on the nine-point scale, moving the shoulder from neutrality to slightly warm.

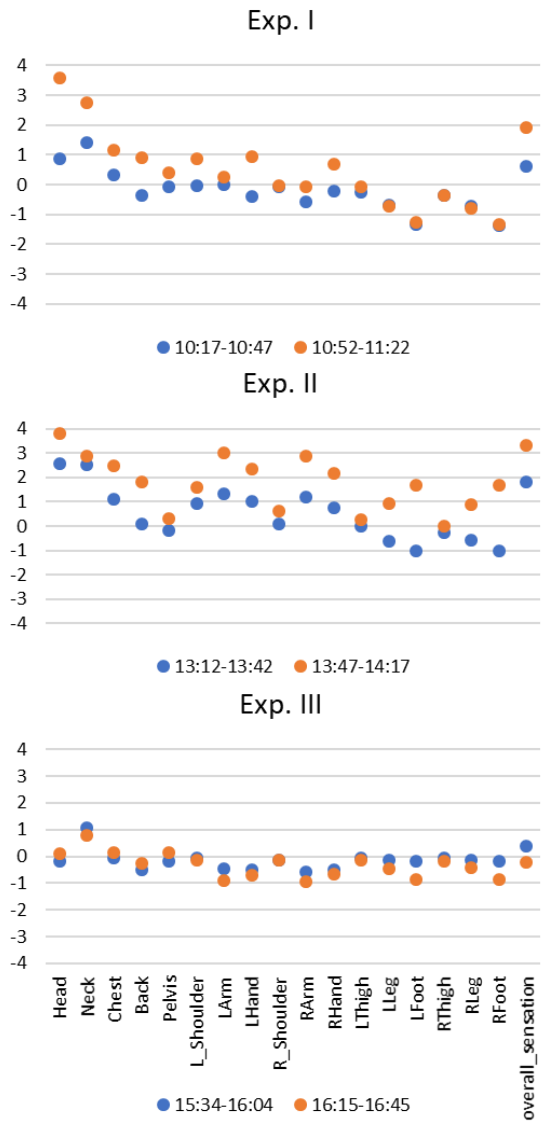

Fig. 6 Local thermal sensation and overall sensation prediction over the different experimental sessions.

4. Discussion

Based on the local skin temperature, it is clear that the effect of solar radiation had more influence on the left part of the subject. The shoulders showed the highest difference in experiment II-b, where the solar intensity was the highest. The differences between left and right were clearer in the simulation from Experiment I-b, especially between the arms and shoulders. During the experiment, the subject conducted a survey of thermal sensation and thermal comfort. From his voting, it seems the environment was neutral in both exp. I and III, but exp. II showed a warmer sensation. The subject felt warm in the following body parts: head, chest, back, left shoulder, left arm, and left hand. Based on the thermal sensation results, we can see that the simulation indicated a warm environment in the second half of the experiment I, overall sensation in experiment II, showed warm and hot results. In the third experiment, the results showed a neutral thermal sensation, which is expected due to the non-presence of solar radiation. In general, the results comparison shows that although there are some discrepancies in the local results, the model still follows the physiological response behaviour of the human subject.

5. Conclusion

The indoor environment is heterogeneous and non-uniform, and consequently, accounting for the non-homogeneous nature of the environment in the design process increases the accuracy and the expectation of the design. The heat stress that can occur as a result of direct exposure to solar radiation places the occupant in an uncomfortable situation. Even in the case of partial body exposure to solar radiation, this can affect the whole-body thermal state, as our results showed. This paper presented a detailed approach to calculating the local MRT of a person seated close to a window.

The simulation results showed an acceptable correlation with the experimental results. Even so, there is still room for improvement in order to achieve better accuracy. For instance, the model needs to be tested on multiple subjects, for which different subjects need to be included in the experiment. Moreover, the MRT calculation was happening every 30 minutes, and that could be improved by shortening the duration to 10 minutes in order to better account for the variability of the environment. A thorough investigation and development needs to be conducted on the human thermo-physiology model in order to achieve better accuracy in local skin temperature as some body parts showed higher values compared to the experimental ones.

6. References

[1] Arens E, Hoyt T, Zhou X, et al. (2015). Modeling the comfort effects of short-wave solar radiation indoors. Building and Environment, 88: 3–9.

[2] Arens E, Heinzerling D, Paliaga PE (2018). Sunlight and indoor thermal comfort. ASHRAE Journal, 2018(7): 12–21.

[3] La Gennusa, M., Nucara, A., Pietrafesa, M., & Rizzo, G. (2007). A model for managing and evaluating solar radiation for indoor thermal comfort. Solar Energy, 81(5), 594-606.

[4] ISO, ISO7730. "7730: Ergonomics of the thermal environment Analytical determination and interpretation of thermal comfort using calculation of the PMV and PPD indices and local thermal comfort criteria." Management 3.605 (2005): e615.

[5] Zhang, H. (2003). Human thermal sensation and comfort in transient and non-uniform thermal environments. University of California, Berkeley.

[6] Staiger, H., & Matzarakis, A. (2020). Accuracy of Mean Radiant Temperature Derived from Active and Passive Radiometry. Atmosphere, 11(8), 805.

[7] Takahashi, Y., Nomoto, A., Yoda, S., Hisayama, R., Ogata, M., Ozeki, Y., & Tanabe, S. I. (2021). Thermoregulation model JOS-3 with new open source code. Energy and Buildings, 231, 110575.

[8] Huizenga, C., Hui, Z. and Arens, E., 2001. A model of human physiology and comfort for assessing complex thermal environments. Building and Environment, 36(6), pp.691-699.

[9] KINGMA, B. R. M. Human thermoregulation: a synergy between physiology and mathematical modelling. 2012.

[10] Tanabe, S. I., Kobayashi, K., Nakano, J., Ozeki, Y., & Konishi, M. (2002). Evaluation of thermal comfort using combined multi-node thermoregulation (65MN) and radiation models and computational fluid dynamics (CFD). Energy and Buildings, 34(6), 637-646.

[11] Fiala, D., Lomas, K. J., & Stohrer, M. (1999). A computer model of human thermoregulation for a wide range of environmental conditions: the passive system. Journal of applied physiology, 87(5), 1957-1972.

[12] Stolwijk, J.A., 1971. A mathematical model of physiological temperature regulation in man (No. NASA-CR-1855). NASA.

[13] Aviv, D., Gros, J., Alsaad, H., Teitelbaum, E., Voelker, C., Pantelic, J., & Meggers, F. (2022). A data-driven ray tracing simulation for mean radiant temperature and spatial variations in the indoor radiant field with experimental validation. Energy and Buildings, 254, 111585.

[15] Guo, H., Aviv, D., Loyola, M., Teitelbaum, E., Houchois, N., & Meggers, F. (2020). On the understanding of the mean radiant temperature within both the indoor and outdoor environment, a critical review. Renewable and Sustainable Energy Reviews, 117, 109207.